

An empirical appraisal of methods for the dynamic prediction of survival with numerous longitudinal predictors

Mirko Signorelli¹ and Sophie Retif²

¹*Mathematical Institute, Leiden University (NL)*

²*School of Industrial and Information Engineering, Politecnico di Milano (IT)*

Abstract

Recently, the increasing availability of repeated measurements in biomedical studies has motivated the development of several statistical methods for the dynamic prediction of survival in settings where a large (potentially high-dimensional) number of longitudinal covariates is available. These methods differ in both how they model the longitudinal covariates trajectories, and how they specify the relationship between the longitudinal covariates and the survival outcome. Because these methods are still quite new, little is known about their applicability, limitations and performance when applied to real-world data.

To investigate these questions, we present a comparison of the predictive performance of the aforementioned methods and two simpler prediction approaches to three datasets that differ in terms of outcome type, sample size, number of longitudinal covariates and length of follow-up. We discuss how different modelling choices can have an impact on the possibility to accommodate unbalanced study designs and on computing time, and compare the predictive performance of the different approaches using a range of performance measures and landmark times.

Keywords: dynamic prediction; survival analysis; longitudinal data; risk prediction modelling.

1 Introduction

Estimating the probability that individuals may experience adverse events (e.g., onset of a disease or death) is an important task of modern medicine. Risk prediction models (Steyerberg, 2009) are statistical and machine learning models that can be employed to estimate the probability that each individual will experience a certain event over time. Risk prediction models can be used by clinicians to monitor disease progression, provide

patients with information about their health status and risks, and guide decisions about hospitalization, surgeries and initiating, adjusting or terminating a certain treatment. A common approach to risk prediction modelling involves estimating the probability that individuals will not experience the event over time (called *survival probability*) based on a set of risk factors (*covariates*) that are either time-independent, i.e. do not change over time or are measured at a single time point. The main advantages of this static modelling approach are that it is relatively easy to implement and it does not require gathering patient information over time. However, predictions developed in this way do not incorporate any information on individual changes over time that may be predictive of the event of interest. If such information is deemed relevant for the occurrence of the event, then ideally we would like to measure time-varying covariates at multiple points in time, and to incorporate information from such repeated measurements in the prediction model to improve predictive accuracy. Moreover, we would like to be able to dynamically update individual predictions of survival each time new (more recent) measurements become available.

Traditional approaches to the dynamic prediction of survival include landmarking (Van Houwelingen, 2007) and joint modelling (Rizopoulos, 2012). Landmarking requires the specification of a so-called landmark time. Individuals that experienced the event or were censored before the landmark are discarded, so that modelling is restricted to individuals who survived up to the landmark time. Then, for each longitudinal covariate a summary measure is computed from all repeated measurements up to the landmark time, and the summary measures thus computed are used as predictors in a Cox proportional hazards model. In the simplest approach, called last observation carried forward (LOCF) landmarking, the last observation of each longitudinal covariate before the landmark time is used as summary measure. The major advantages of the LOFC approach are its simplicity and ease of implementation; possible disadvantages include the fact that the last observation taken before the landmark may be outdated, and the lack of a model to describe the evolution over time of the longitudinal covariates and to account for measurement error (which may be considerable in the case of biomarkers). Joint modelling involves the specification and estimation of a shared random effects model for both the longitudinal covariates and the survival outcomes. Its estimation is typically computationally demanding, and this has so far restricted the applicability of joint models to problems with only one or at most a handful of longitudinal covariates. Recently, Putter and van Houwelingen (2022) proposed a “landmarking 2.0” approach that tries to combine different aspects of landmarking and JMs, focusing on a situation with only one longitudinal biomarker.

Over the last decades, technological advancements have led to an increasing availability of studies where many longitudinal covariates are measured alongside with a survival outcome. Examples of such studies include observational studies where patients are monitored for several years to study the occurrence of a slowly progressing disease such as cancer (Patel et al., 2017), dementia (Bennett et al., 2018) or Alzheimer’s disease (Weiner et al., 2010), as well as studies focused on the identification of biomarkers associated with disease progression and the occurrence of disease milestones among a

large number of longitudinal omic (e.g., protein, gene or metabolite expression levels) markers (Signorelli et al., 2020; Filbin et al., 2021).

Recently, this increasing availability of repeated measurement data in biomedical studies has motivated the development of new statistical methods that can be used for the dynamic prediction of survival in situations where a large (potentially high-dimensional) number of longitudinal covariates is available. These approaches differ in the way in which they model the evolution over time of the longitudinal covariates, as well as in the way in which they model the relationship between summaries of the longitudinal covariates and the survival outcome. Li and Luo (2019) proposed the Multivariate Functional Principal Component Analysis Cox model (MFPCCoX), which employs multivariate functional principal component analysis (MFPCA) to summarize the longitudinal covariates, and then uses the MFPCA scores as covariates in a Cox model for the survival outcome. Signorelli et al. (2021) proposed Penalized Regression Calibration (PRC), which uses linear as well as multivariate mixed-effects models to model the trajectories of the longitudinal predictors, and predicts the survival outcome with a penalized Cox model where the predicted random effects are included as covariates. Although Signorelli et al. (2021) did not consider a dynamic prediction setup, the use of PRC for dynamic prediction was later illustrated in Signorelli (2023). Lin et al. (2021) proposed the Functional Random Survival Forest (FunRSF) approach, where longitudinal covariates are modelled through MFPCA similarly to MFPCCoX, and the MFPCA scores are then used as time-fixed covariates to predict survival with a random survival forest. Lastly, Devaux et al. (2022) proposed a dynamic Random Survival Forest (DynForest) method that uses linear mixed models (LMMs) to summarize the longitudinal covariates, and then uses the predicted random effects as time-fixed covariates within a random survival forest.

Because these new methods were proposed in the last few years, to date little is known about their applicability to, and performance with, real-world datasets. Practical modelling questions include how well each method can accommodate datasets with unbalanced repeated measurements, and how computationally intensive each method is as a function of the sample size and number of longitudinal covariates (specially when compared to a computationally inexpensive approach such as landmarking and to a computationally inefficient one such as JM). Furthermore, it is of primary interest to evaluate the predictive performance of these alternative modelling approaches on multiple real-world datasets with different features.

To investigate these questions, we gathered data from three longitudinal studies that differ in terms of outcome type, sample size, number of longitudinal covariates and length of follow-up. We applied MFPCCoX, PRC, FunRSF and DynForest, alongside two simpler prediction approaches, to each dataset, and proceeded to evaluate the predictive performance of each method according to three different metrics for survival data.

The remainder of this article is organized as follows: in Section 2 we briefly describe the problem of dynamic prediction and the methods considered in our empirical comparison. In Section 3 we present the 3 datasets included in our comparison alongside with

information about how the prediction methods were applied to each dataset. Section 4 describes the results of the comparison, whereas Section 5 contains some discussion points and concluding remarks.

2 Methods for the dynamic prediction of survival

2.1 Dynamic prediction of survival

We consider the setup of a longitudinal study where n subjects are enrolled, and interest lies in predicting the occurrence of a certain event of interest for the different individuals. Each subject $i \in \{1, 2, \dots, n\}$ is followed from time $t = 0$ (study entry) until they either experience the event of interest at time t_i , or they are right-censored at time c_i . We denote by T_i and C_i the random variables corresponding to the event and censoring times, respectively, and let $T_i^* = \min(T_i, C_i)$. Furthermore, we denote by t_i^* the observed value of T_i^* for subject i , and introduce a censoring indicator δ_i that is 1 if for subject i the event of interest is observed at $t_i^* = t_i$, and 0 in case of censoring, i.e. if the event has not yet been observed at $t_i^* = c_i$.

Between times 0 and t_i^* , subject i undergoes $m_i \geq 1$ visits at times $t_{i1}, t_{i2}, \dots, t_{im_i}$, where we assume that $t_{i1} = 0$, $t_{i1} < t_{i2} < \dots < t_{im_i}$ and $t_{im_i} < t_i^*$. At time $t_{i1} = 0$, P baseline covariates $x_i = (x_{1i}, \dots, x_{Pi})$ are measured. Moreover, Q longitudinal covariates are measured at each follow-up visit (including $t_{i1} = 0$). We equivalently denote by $y_{qij} = y_{iq}(t_{ij})$ the value of the q -th longitudinal covariate measured on subject i at time t_{ij} , and let $y_{ij} = y_i(t_{ij}) = (y_{1ij}, \dots, y_{Qij})$ be the corresponding Q -dimensional vector.

Let $\mathcal{I}(t) = \{i \in \{1, 2, \dots, n\} : t_i^* > t\}$ denote the set of individuals that are still at risk at a given time point t . Moreover, let $\mathcal{H}_i(t) = (x_i, y_i(0), \dots, y_i(t_{ik}))$, where k is such that $t_{ik} \leq t < t_{i,k+1}$, denote the covariate information available for a subject $i \in \mathcal{I}(t)$ up until time t (in other words, $\mathcal{H}_i(t)$ contains both the P baseline covariates, and all repeated measurements taken up until time t of the Q longitudinal covariates).

At any point in time $t_1 \in (0, t_i^*)$, we may want to predict the conditional probability $P(T_i > t_2 | T_i > t_1)$ that individual i will still be event-free at time t_2 , given that they had not experienced the event at $t_1 < t_2$. More specifically, given a so-called *landmark time* ℓ , our goal is to estimate the conditional survival function

$$S_i(t|\ell, \mathcal{H}_i(\ell)) = P(T_i > t | T_i > \ell, \mathcal{H}_i(\ell)), \quad i \in \mathcal{I}(\ell), \quad t \geq \ell, \quad (1)$$

using all the baseline and longitudinal covariate information $\mathcal{H}_i(\ell)$ available up until ℓ for subjects $i \in \mathcal{I}(\ell)$.

In dynamic prediction, it can often be of interest to compute predictions of survival $S_i(t|\ell_k, \mathcal{H}_i(\ell_k))$ over a range of K landmark times $\ell_1, \ell_2, \dots, \ell_K$, rather than for a single landmark ℓ ; if that is indeed the case, our notation can be easily adjusted by re-defining $\mathcal{I}(\ell_k)$ and $\mathcal{H}_i(\ell_k)$ for each landmark time ℓ_k .

2.2 Strict vs relaxed landmarking of the longitudinal data

Equation (1) states that the goal of dynamic prediction is to predict the probability of survival for those individuals that survived past the landmark time ℓ , using as predictors all covariate values measured up to time ℓ .

When estimating a statistical model to address the dynamic prediction problem at time ℓ , one would usually estimate the prediction model using only those covariate values contained in $\mathcal{H}_i(\ell)$, discarding any repeated measurement taken after ℓ as such measurements would not be available to compute predictions at the prediction time ℓ . Gomon et al. (2024) named this approach “strict landmarking”, contrasting it to a “relaxed landmarking” approach where the model is estimated including longitudinal measurements taken after ℓ for all subjects in the training set.

In the literature, dynamic prediction methods are often estimated using the relaxed data landmarking approach, probably because such approach allows to use more repeated measurements to model the trajectories of the longitudinal data. However, relaxed data landmarking can be problematic for two reasons: first, it uses future information (collected after $t > \ell$) to predict the conditional survival probability $P(T > t | T > \ell)$. Note that such future information is not available at the landmark time, and thus in reality it would not be possible to make use of it to make predictions at ℓ . Second, relaxed data landmarking introduces a selection bias in the modelling of the longitudinal trajectories: because individuals who survive longer are likely to have more repeated measurements taken after ℓ than individuals with shorter survival, the available measurements after the landmark are not a representative sample from the population of individuals who survived up until ℓ . Whereas this is not an issue with joint models, the two-step approaches considered in this article do not correct for this source of bias. In practice, this means that even though relaxed data landmarking allows to use more data to train these two-steps prediction models, in practice it introduces selection biases that can severely undermine predictive performance. Gomon et al. (2024) compared strict and relaxed data landmarking for the MFPCox method, showing how models trained with a strict data landmarking approach have superior predictive performance over models trained with relaxed data landmarking. Based on the aforementioned remarks and the results of Gomon et al. (2024), hereafter we describe and implement the dynamic prediction models included in our comparison using a strict data landmarking approach.

2.3 Methods for dynamic prediction

2.3.1 Static Cox model

Before describing the dynamic prediction methods compared in this work, we consider a static Cox model (Cox, 1972) that only uses baseline information to predict $S_i(t|\ell, \mathcal{H}_i(\ell))$:

$$h_i(t) = h_0(t) \exp \{ \alpha x_i + \gamma y_i(0) \}, \quad i \in \mathcal{I}(\ell), \quad (2)$$

where $h_i(t)$ denotes the hazard for subject i at time t , $h_0(t)$ is a non-parametric baseline hazard, and α and γ are vectors of regression coefficients. Model (2) can be estimated using the R package `survival` (Therneau and Grambsch, 2000). The predicted conditional survival probability of equation (1) can be estimated by computing

$$\hat{S}_i(t|\ell, \mathcal{H}_i(\ell)) = \exp \left\{ - \int_0^t h_0(v) e^{\hat{\eta}_i} dv \right\}, \quad (3)$$

where $\hat{\eta}_i$ is the estimated linear predictor for subject i from model (2).

Admittedly, model (2) does not make use of the available longitudinal measurements to update predictions of survival: nevertheless, it is useful to evaluate the predictive performance of such model to quantify how accurate our predictions of survival would be if we were to ignore any information collected after study entrance. By comparing the performance of this static prediction model to that of dynamic methods, which incorporate more and more repeated measurements as the landmark time increases, we can effectively quantify the extent to which adding longitudinal information to a prediction model may improve predictive performance. Although the discrepancy between static and dynamic methods will be typically data-dependent, in general we can expect the difference between these two approaches to increase as the landmark time increases, as the information provided to model (2) becomes more and more outdated, while dynamic methods continue being fed more and more up to date patient information.

2.3.2 Landmarking

Landmarking (Van Houwelingen, 2007) is a pragmatic approach to dynamic prediction that summarizes the trajectory of each longitudinal covariate up until the landmark time into a single summary measure per covariate. Two commonly-used summary measures are the last available observation (up to ℓ) of the longitudinal covariate, an approach referred to as *last observation carried forward (LOCF)*, and the average of all repeated measurements taken up until ℓ . The summaries of the longitudinal covariates are then included as predictors in a Cox model alongside with the baseline covariates. The LOCF landmarking method can be formalized as follows. For each subject $i \in \mathcal{I}(\ell)$ and each longitudinal covariate $q \in \{1, \dots, Q\}$, consider the full trajectory $y_{qi} = (y_{qi1}, y_{qi2}, \dots, y_{qim_i})$ and denote by y_{qi}^ℓ the last non-missing value y_{qik} in y_{qi} such that $t_{ik} \leq \ell$ (notice that if there are no missing values in y_{qi} for every q , then the measurement times of y_{qi}^ℓ are the same across q , otherwise they may differ). The LOCF approach involves fitting the Cox model

$$h_i(t) = h_0(t) \exp \left\{ \alpha x_i + \sum_{q=1}^Q \gamma_q y_{qi}^\ell \right\}, \quad i \in \mathcal{I}(\ell), \quad (4)$$

where α and $\gamma = (\gamma_1, \gamma_2, \dots, \gamma_Q)$ are vectors of coefficients.

The LOCF landmarking model can be easily estimated using existing software for survival analysis, such as the R package `survival` (Therneau and Grambsch, 2000). The predicted survival for subject i can be estimated using equation (3), where now $\hat{\eta}_i$ is the estimated linear predictor for subject i from model (4).

2.3.3 Multivariate Functional Principal Component Analysis Cox model (MFPCCoX)

The Multivariate Functional Principal Component Analysis Cox (MFPCCoX) model (Li and Luo, 2019) is a prediction approach that uses Multivariate Functional Principal Component Analysis (MFPCA) to summarize the Q longitudinal covariates into MFPCA scores, which are then used as predictors of survival in a Cox model.

First, MFPCA (Happ and Greven, 2018) is employed to approximate the longitudinal trajectory for the q -th longitudinal predictor as the sum of a mean process $\mu_q(t)$ shared by all subjects, and a finite sum of subject-specific MFPCA scores ρ_{ki} that are shared across the Q longitudinal covariates:

$$y_{qij} = y_{qi}(t_{ij}) \approx \mu_q(t_{ij}) + \sum_{k=1}^K \rho_{ki} \psi_{kq}(t_{ij}), \quad i \in \mathcal{I}(\ell), \quad t_{ij} \leq \ell, \quad (5)$$

where $\psi_k(t) = (\psi_{k1}(t), \dots, \psi_{kQ}(t))$ are Q -variate orthonormal eigenfunctions with associated MFPCA scores ρ_{ki} . The eigenfunctions are ordered by decreasing percentage of variance explained, and K is chosen in such a way that the first K eigenfunctions explain a certain proportion of the variance of the longitudinal covariates.

To predict survival, MFPCCoX uses the estimated MFPCA scores for subject i as summaries of all repeated measurements of the longitudinal covariates, including the MFPCA scores alongside the baseline covariates as predictors in a Cox model:

$$h_i(t) = h_0(t) \exp \left\{ \alpha x_i + \sum_{k=1}^K \gamma_k \hat{\rho}_{ki} \right\}, \quad i \in \mathcal{I}(\ell), \quad (6)$$

where $\hat{\rho}_{ki}$ are the estimated MFPCA scores, and α and $\gamma = (\gamma_1, \gamma_2, \dots, \gamma_K)$ are vectors of coefficients. MFPCCoX can be estimated using the R code provided in Li and Luo (2019). The predicted survival for subject i can be estimated using equation (3), where $\hat{\eta}_i$ is now the estimated linear predictor for subject i from model (6).

2.3.4 Penalized Regression Calibration (PRC)

The Penalized Regression Calibration (PRC) method (Signorelli et al., 2021) uses mixed-effects models to summarize the Q longitudinal covariates into predicted random effects, which are then used as predictors of survival in a Cox model.

First, PRC models each longitudinal covariate (or a transformed version of it, for example its log-transform) using a linear mixed effects model (LMM, McCulloch and Searle 2004):

$$y_{qij} = y_{qi}(t_{ij}) = W_{qi}(t_{ij})\beta_q + Z_{qi}(t_{ij})u_{qi} + \varepsilon_{qij}, \quad i \in \mathcal{I}(\ell), \quad t_{ij} \leq \ell, \quad (7)$$

where β_q is a vector of population parameters shared across all subjects called *fixed effects*, u_{qi} is a vector of subject-specific parameters called *random effects* that are assumed to follow a multivariate normal distribution, ε_{qij} is a vector of Gaussian errors, and $W_{qi}(t_{ij})$ and $Z_{qi}(t_{ij})$ are design matrices containing the covariates relevant for β_q and u_{qi} respectively. Signorelli et al. (2021) also consider an alternative, more complex multivariate mixed model, which is not relevant for our model benchmarking. Specifically, in this article we consider a LMM with a random intercept and a random slope that depends on time t_{ij} :

$$y_{qij} = \beta_{q0} + u_{qi0} + \beta_{q1}t_{ij} + u_{qi1}t_{ij} + \varepsilon_{qij}, \quad i \in \mathcal{I}(\ell), \quad t_{ij} \leq \ell, \quad (8)$$

where $\beta_q = (\beta_{q0}, \beta_{q1})$, $u_{qi} = (u_{qi0}, u_{qi1})^T \sim N(0, \Sigma_q)$, and $\varepsilon_{qi} \sim N(0, \sigma_q^2 I)$. Notice that although Signorelli et al. (2021) and Signorelli (2023) suggest to employ age at observation as time covariate in equation (8), here we choose to model y_{qij} as a function of time on study t_{ij} to make PRC directly comparable with MFPCox, FunRSF and DynForest, as all of those methods model y_{qij} on the time on study scale.

After model (7) has been estimated, a vector \hat{u}_{qi} with the predicted random effects for covariate q and subject i is computed. In the case of model (8), that means that the predicted random intercept \hat{u}_{qi0} and slope \hat{u}_{qi1} are obtained as summaries of the vector y_{qi} . To predict survival, PRC uses a Cox model where the predicted random effects are used as predictors of survival together with the baseline covariates:

$$h_i(t) = h_0(t) \exp \left\{ \alpha x_i + \sum_{q=1}^Q \gamma_q \hat{u}_{qi0} + \sum_{q=1}^Q \theta_q \hat{u}_{qi1} \right\}, \quad i \in \mathcal{I}(\ell), \quad (9)$$

where \hat{u}_{qi0} and \hat{u}_{qi1} denote the estimated random effects from model (8), and $\alpha, \gamma = (\gamma_1, \dots, \gamma_Q)$ and $\theta = (\theta_1, \dots, \theta_Q)$ are vectors of regression coefficients. Model (9) is estimated using penalized maximum likelihood.

The PRC method can be estimated using the R package `pencal` (Signorelli, 2023). For PRC, the predicted survival for subject i can be estimated using equation (3), where $\hat{\eta}_i$ denotes the estimated linear predictor for subject i from model (9).

2.3.5 Functional Random Survival Forest (FunRSF)

The Functional Random Survival Forest (FunRSF) (Lin et al., 2021) approach uses MFPCA to summarize the trajectories described by the longitudinal covariates, and random survival forests to predict survival. The MFPCA modelling step is analogous to the one used by MFPCox and described in equation (5). This step will yield a set of K estimated MFPCA scores $\hat{\rho}_{ki}, k = 1, \dots, K$ for each subject $i \in \mathcal{I}(\ell)$, which are then used within a random survival forest (RSF, Iswaran et al., 2008) algorithm as time-independent covariates together with the baseline covariates x_i .

The estimation of the RSF involves sampling B bootstrap samples from a dataset that comprises information on the survival outcome, the baseline covariates and the MFPCA scores. For each bootstrap sample, a random survival tree is estimated, using as splitting variables both the baseline covariates and the MFPCA scores. At each node of the tree, a fixed number F of candidate splitting variables is selected among the union of the P baseline covariates and K MFPCA score variables. Each node is split by identifying the candidate variable whose splitting maximizes the log-rank test statistic, and the splitting is continued until a terminal node is reached. A node is terminal if further splitting would lead to child nodes that contain less than a fixed number s of subjects (notice that both F and s are tuning parameters that can be determined by the user). Each terminal node k in the b -th tree is then summarized by its cumulative hazard function (CHF) $\hat{H}_{bk}(t|\ell)$. The estimated CHF for subject i is obtained by dropping i through each tree to obtain its estimated CHF $\hat{H}_b(t|\ell, x_i, \hat{\rho}_i)$, and then averaging over the B bootstrap samples to obtain the "ensemble" CHF estimate

$$\hat{H}(t|\ell, x_i, \hat{\rho}_i) = \frac{1}{B} \sum_{b=1}^B \hat{H}_b(t|\ell, x_i, \hat{\rho}_i), \quad (10)$$

which is then used to estimate $\hat{S}_i(t|\ell, \mathcal{H}_i(\ell)) = \exp \left\{ -\hat{H}(t|\ell, x_i, \hat{\rho}_i) \right\}$. MFPCCoX can be estimated using the R code provided in Lin et al. (2021).

2.3.6 Dynamic Random Survival Forest (DynForest)

The Dynamic Random Survival Forest (DynForest, Devaux et al., 2022) method makes use of LMMs to summarize the Q longitudinal covariates into predicted random effects that are used as predictors of survival within a RSF.

The estimation of the RSF starts with B bootstrap samples from a dataset that comprises information on the survival outcome, the baseline covariates and the longitudinal covariates. For each bootstrap sample, a survival tree is estimated as follows: at each node, a fixed number F of candidate splitting variables is selected among the union of the P baseline covariates and the Q longitudinal covariates. For each longitudinal covariate, a linear mixed-effects model of the form given in equation (7) is estimated, and the longitudinal trajectory of covariate q for subject i , y_{qi} , is then summarized by the predicted random effects in the same way as described in Section 2.3.4 for PRC. The predicted random effects from the candidate longitudinal covariates are then used as time-independent covariates alongside with the candidate baseline covariates as possible splitting variables for the given node. Similarly to FunRSF, the node is split choosing the covariate that maximizes the log-rank statistics. The construction of the tree continues until a terminal node that contains a pre-specified number of subjects s , and a prespecified number of events e is reached. Lastly, the estimated CHF for subject i is computed by dropping i down each tree, obtaining their estimated CHF according to the b -th tree, $\hat{H}_b(t|\ell, x_i, y_i)$, and averaging those tree-specific CHFs to obtain the ensemble CHF estimate

$$\hat{H}(t|\ell, x_i, y_i) = \frac{1}{B} \sum_{b=1}^B \hat{H}_b(t|\ell, x_i, y_i), \quad (11)$$

which is then used to estimate $\hat{S}_i(t|\ell, \mathcal{H}_i(\ell)) = \exp \left\{ \hat{H}(t|\ell, x_i, y_i) \right\}$.

Notice that although the construction of the RSF in DynForest shares similarities with FunRSF, an important difference is that FunRSF uses a single MFPCA computation to summarize the longitudinal covariates into MFPCA scores prior to estimating the RSF, whereas DynForest estimates new LMMs within each tree and node (meaning that the same longitudinal covariate may be summarized by different predicted random effects across trees and nodes). In addition, DynForest can be used also in combination with competing risks, which we do not consider in this article as our goal is to compare the predictive performance of the aforementioned methods (most of which have not been developed to incorporate competing risks). The DynForest model can be estimated using the R package `DynForest` (Devaux et al., 2023).

3 Datasets and implementation

Sections 3.1-3.3 present the three datasets considered in this article. For each dataset we describe how the data were gathered, the length of follow-up and the frequency of repeated measurements; then, we define the survival outcome that we want to predict, and list the baseline and longitudinal covariates that are employed to predict it. As it will become apparent later in this section, the three datasets differ substantially in sample size, length of the follow-up, frequency and number of repeated measurements per subject and number of longitudinal covariates employed as predictors, making them representative of different scenarios that one may encounter when dealing with real-world longitudinal studies.

Lastly, in Section 3.4 we provide information about the implementation of the dynamic prediction methods for these datasets, including information about landmark times and prediction horizons, performance measures, tuning parameters and further computational details.

3.1 The ADNI dataset

The Alzheimer’s Disease Neuroimaging Initiative (ADNI) study (Weiner et al., 2010) is an ongoing study started in 2004 that was designed to identify and validate biomarkers related to the progression of AD. By April 2023, the study had enrolled 2428 individuals, each of which is scheduled to undergo an initial visit and subsequent assessments scheduled at 3, 6, 12, 18, 24, 36, and 48 months from baseline, followed by annual visits thereafter. Throughout the follow-up visits participants undergo comprehensive evaluations for dementia, including a variety of cognitive assessments, as well as biospecimen sampling and brain imaging analysis.

Differently from the ROSMAP study that will be introduced in Section 3.2, where the cause of dementia (AD or not AD) is reported, the ADNI study only reports dementia diagnoses, without attributing them to AD or other causes. At each visit, ADNI participants are classified into one of the following categories: cognitive normal (CN), mildly cognitive impaired (MCI), or affected by dementia. Moreover, both baseline information about the participant and longitudinal measurements of cognitive, imaging and biochemical markers are collected in this study.

Our analysis aims to predict the time from baseline until a dementia diagnosis for subjects that entered the study as CN or MCI. To predict this survival outcome we employ 5 baseline covariates (age, gender, baseline diagnosis, number of apolipoprotein $\epsilon 4$ alleles, and number of years of education) and 21 longitudinal covariates that are listed in Supplementary Table 1. These covariates were selected based on their relevance as predictors of dementia and on the fact that they did not have too many missing values.

After removing subjects already diagnosed with dementia at baseline, subjects without any follow-up information after baseline, and subjects with missing covariate values at baseline the baseline visit, 1643 subjects were retained for analysis. The number of visits per subject varies from 1 to 22, with a mean of 6.2 visits. The follow-up period ranges between 3 months and 15.5 years, with a mean of 3.4 years. Supplementary Figure 1 illustrates how number of individuals at risk changes over time, and the Kaplan-Meier estimator of the probability to be free from dementia in the ADNI dataset.

3.2 The ROSMAP dataset

The Religious Orders Study and Rush Memory and Aging Project (ROSMAP) study (Bennett et al., 2018) is an ongoing project designed to study the onset of Alzheimer’s disease (AD). Started in 1994, by May 2023 ROSMAP had enrolled 3757 participants, collecting longitudinal information about their cognitive status and possible risk factors for AD.

Every year, subjects enrolled in ROSMAP undergo a clinical assessment that leads to an evaluation of their cognitive status, which is classified into 6 classes: no cognitive impairment (NCI); mild cognitive impairment (MCI); MCI and another condition contributing to cognitive impairment (MCI+); Alzheimer’s dementia (AD); AD and other condition contributing to CI (AD+); other primary cause of dementia, without clinical evidence of AD (Other). In addition, longitudinal information about a wide range of genomic, experiential, psychological and medical risk factors is collected alongside information (such as age, gender, education) about the participant’s background.

In this article we focus on predicting the time (measured from the date of study enrollment) until AD is diagnosed (i.e. , cognitive status AD or AD+) for subjects that entered the study in the NCI, MCI, MCI+ and Other categories. To do so we employ 5 baseline covariates (age, gender, years of education received, baseline cognitive status and presence of a cancer diagnosis) and a set of 30 longitudinal covariates, listed in

Supplementary Table 2, which measure aspects related to several different domains (these covariates were selected from a larger list of longitudinal covariates both because of their relevance as risk factors for AD, and because they did not have too many missing values).

After removing subjects already diagnosed with AD at baseline, subjects without any follow-up information after baseline, and subjects with missing covariate values at baseline, 3293 subjects were retained for analysis. The number of visits per subject varies from 2 to 30, with a mean of 9.3 visits. The follow-up period ranges between 1 and 29 years, with a mean of 8.3 years. Supplementary Figure 2 illustrates how number of individuals at risk evolves over time, and the Kaplan-Meier estimator of the probability to be free from AD in the ROSMAP dataset.

3.3 The PBC2 dataset

The PBC2 dataset contains data from a clinical trial on primary biliary cholangitis (PBC) conducted between 1974 and 1984 at the Mayo Clinic (Murtaugh et al., 1994). The randomized trial involved 312 participants who were randomized between a treatment group where patients received the drug D-penicillanime and a placebo group. The trial recorded the occurrence of the first of two survival outcomes: liver transplantation, or death. Because most of the methods considered in our comparison cannot deal with competing risks, for the purpose of our analysis we focus on predicting time to death, treating patients who underwent liver transplantation as right-censored at the date of transplantation.

To predict time to death, we employ 3 baseline covariates (age, gender and treatment group) alongside with the 8 longitudinal covariates listed in Supplementary Table 3. Patients enrolled in the trial underwent visits upon study entry, 6 and 12 months after baseline, and yearly visits after that. The number of follow-up visits per patient ranged between 1 and 22, with an average of 6.1; the follow-up period ranged from 0.1 to 14.1 years, with a mean of 4.6 years. Supplementary Figure 3 shows the number of patients at risk and the Kaplan-Meier estimator of the survival probability for the PBC2 dataset.

3.4 Application of the dynamic prediction methods to the ROSMAP, ADNI and PBC2 datasets

3.4.1 Definition of the landmark and horizon times

The datasets considered in our study differ substantially in their sample size, frequency of the repeated measurements (visits) and length of the follow-up. All of these aspects affect both the number of individuals still at risk at a given landmark, and the number of repeated measurements per subject available up to the landmark time. Lastly, the length of the follow-up across patients affects the possibility to evaluate predictive performance at a given horizon.

For these reasons, we determined the landmark and horizon times at which predictions of survival are evaluated separately for each dataset, trying to balance the need to have a good number of repeated measurements to model the evolution of the longitudinal covariates with MFPCA or LMMs, and that of having a good number of individuals still at risk to be able to estimate the Cox / RSF model and reliably assess predictive performance. Clearly, this is easier for the ADNI and ROSMAP datasets, whose sample sizes are considerably bigger than that of PBC2.

The landmarks considered in our analysis are the following:

1. ADNI: 2, 3 and 4 years from baseline;
2. ROSMAP: 2, 3, 4, 5 and 6 years from baseline;
3. PBC2: 2.5, 3 and 3.5 years from baseline.

The accuracy of predictions was evaluated for every year after the landmark up to 10 years from baseline for ADNI, up to 15 years from baseline for ROSMAP, and up to 8 years from baseline for PBC2.

3.4.2 Performance measures and validation of predictive performance

To evaluate the predictive accuracy of the different models we computed the following performance measures for survival data: the Brier score (Graf et al., 1999), the time-dependent AUC (Heagerty et al., 2000), and the C index (Pencina and D’Agostino, 2004). We employed *repeated* cross-validation (CV) to obtain unbiased estimates of the predictive performance of the different models. For the ROSMAP and ADNI datasets we employed 10-fold CV with 10 repetitions; for the PBC2 dataset, where using 10-fold CV led to very small validation folds that would have resulted in unreliable estimates of predictive performance, we employed 5-fold CV with 20 repetitions.

3.4.3 Implementation details

In order to guarantee a fair comparison of the methods included in the analysis, all methods were trained on data from the same set of subjects. Specifically, we excluded from the datasets subjects for which either (a) the value of one or more baseline covariates was missing or (b) the value of one of the longitudinal predictors at the baseline visit was missing to avoid the need of multiple imputation that, given the small number of subjects for which this happened, would have unnecessarily complicated our analyses. While (a) is important for all methods, (b) was added as filtering criterion to ensure that there are no missing values when estimating the static Cox model.

In addition, the 4 methods that model the evolution of the longitudinal predictors over time required additional preprocessing.

Both MFPCox and FunSRF use MFPCA to reduce the longitudinal covariates to MFPCA scores. The estimation of such scores relies on the so-called ”PACE algorithm”, which estimates the univariate FPCA scores from each longitudinal variable

by assuming that the measurements have been obtained using a grid that is regular across subjects. Unfortunately, in the real-world datasets that we consider such assumption is not met, as often visits do not happen exactly at the pre-planned time but may take place a few days / months earlier or later. To overcome this issue, we “regularized” the measurement times across subjects by aligning all visits to the preplanned visit schedule of the specific dataset.

DynForest and PRC employ LMMs to summarize the longitudinal covariates into predicted random effects. Estimation of LMMs can often lead to convergence problems when the response variable is strongly skewed. This can be problematic in our method comparison, where we need to be able to estimate these LMMs several times during the repeated CV. To reduce the frequency of such convergence problems and the need to address convergence issues with ad-hoc solutions each time they arise, we proceeded to apply a log-transformation to those longitudinal covariates whose skewness index was larger than 1, and a cubic transformation to those with skewness index below -1. Furthermore, many of the methods involved in our comparison require the specification of one or more tuning parameters:

- the MFPCA step within MFPCCoX and FunSRF requires the specification of the minimum percentage of variance explained (PVE) to retain when reducing the longitudinal covariates to univariate FPCA scores (PVE_1) and then from univariate to multivariate FPCA scores (PVE_2). We proceeded to set $PVE_1 = PVE_2 = 90\%$;
- PRC allows to choose between the ridge, elasticnet and lasso penalty. We employed the ridge penalty (`penca1`’s default), and used the pre-implemented cross-validation to determine the value of the tuning parameter of the ridge penalty;
- the RSF within FunRSF requires the specification of several parameters. The random forests were trained using an ensemble of $B = 1000$ trees. The hyperparameters of each tree were selected taking into account the specificities of each dataset. The minimum number of subject in a terminal node s was required to be at least 15 for all the datasets. The number of predictors F to be randomly selected at each node was set to the square root of the total number of predictors available in the given dataset;
- the random forests within DynForest were trained using $B = 200$ trees as estimating DynForest is much more time-consuming than estimating FunSRF. Setting the tuning parameters F , s and e for this method is more complicated than for FunRSF, as the need to re-estimate the LMMs after each node split often leads to convergence problems. For this reason, multiple values of s were sequentially tried in case of convergence problems (Supplementary Table 4), progressively increasing s to reduce the chance of encountering convergence errors towards the end of the tree. The value of F was set in the same way as with FunRSF; e was set equal to 5 for ROSMAP and ADNI, and to 4 for PBC2.

4 Results

4.1 ADNI

The repeated CV estimates of the C index, tdAUC and Brier score for the dynamic prediction of time to dementia in the ADNI study are presented in Table 1 and in Figures 1 and 2.

C index. As shown in Table 1, for all landmark times PRC achieves the highest performance, and FunRSF the lowest one. The relative performance of the other methods slightly changing across landmarks: at landmarks 2 and 3, landmarking and static Cox have the second and third highest C index, and are followed by DynForest and MFPCox. Instead, at landmark 4 DynForest is the second best method. Overall, the relative performance of DynForest and MFPCox improves as the landmark time increases, whereas that of landmarking and static Cox worsens.

Method	Landmark		
	2	3	4
Static Cox	0.901 (0.002)	0.885 (0.006)	0.856 (0.008)
Landmarking	0.906 (0.001)	0.89 (0.004)	0.855 (0.009)
MFPCox	0.889 (0.003)	0.872 (0.009)	0.859 (0.008)
PRC	0.913 (0.001)	0.908 (0.003)	0.904 (0.003)
FunRSF	0.873 (0.004)	0.858 (0.011)	0.845 (0.012)
DynForest	0.891 (0.003)	0.883 (0.005)	0.871 (0.011)

Table 1: Cross-validated C index estimates (and standard deviation) for the ADNI dataset

Time-dependent AUC. Overall, the results for the tdAUC (Figure 1) are very much in line with the ones for the C index: PRC is again the best performing method, and FunRSF the worse. Landmarking is the second best at landmark 2, and DynForest at 4; the two methods have similar performance at landmark 3. MFPCox and FunRSF typically show lower accuracy; compared to the other methods, the performance of LOCF landmarking and of the Static Cox model tends to worsen as the landmark increases.

Brier score. In general, the difference in performance across methods appears to be smaller when considering the Brier score (Figure 2). At all landmarks, the static Cox model performs quite well for predictions until year 7; from year 8, its performance starts to worsen in comparison to other methods. PRC is usually the best or second best performing method, followed by landmarking, DynForest and MFPCox. Once again, FunRSF performs worse than all other methods.

Summary. The performance results for the ADNI dataset point out some interesting trends:

- A1) landmarking and the static Cox model show overall a decent performance, specially at earlier landmark times. Surprisingly, these methods often outperform

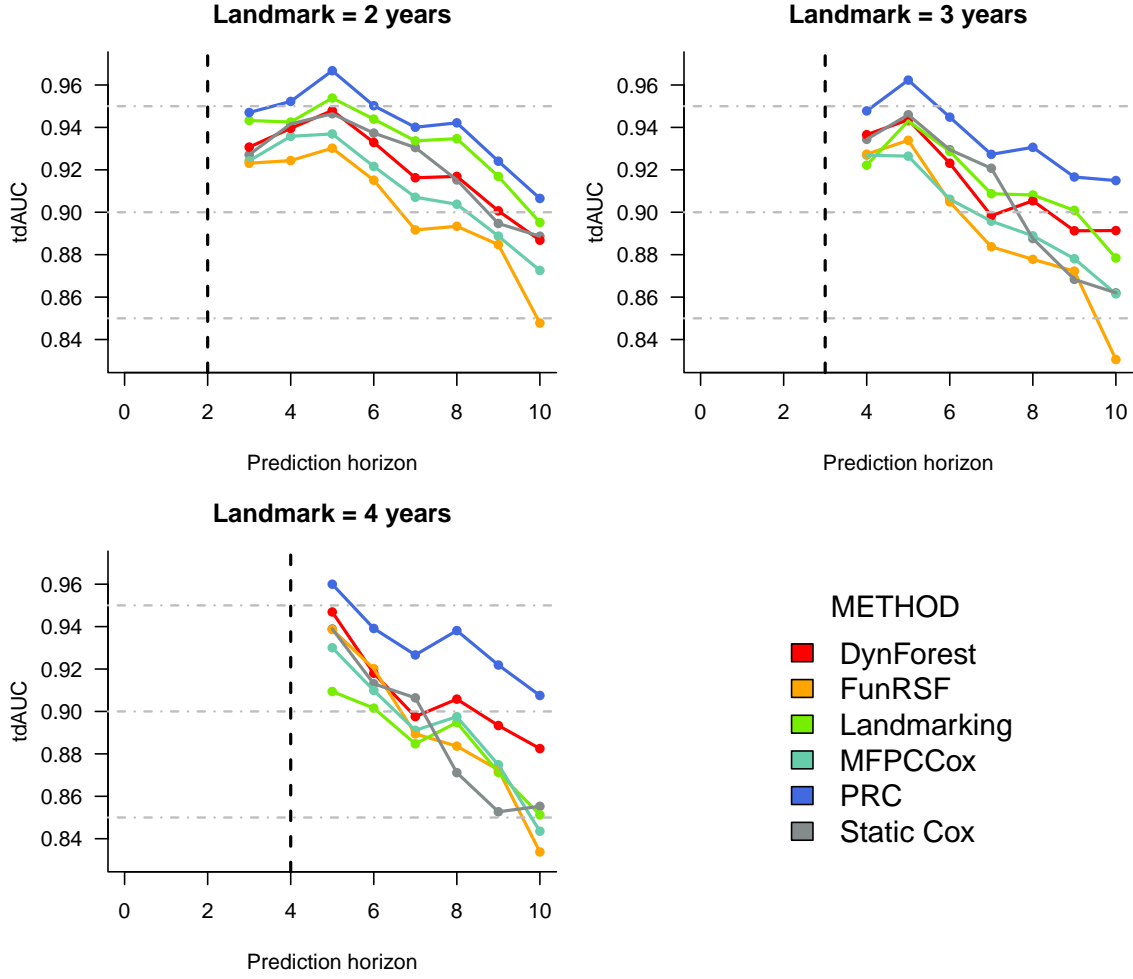


Figure 1: Cross-validation estimates of the time-dependent AUC for the prediction of time to dementia in the ADNI dataset. The corresponding numeric values can be found in Supplementary Table 5.

MFPCox, and always outperform FunRSF;

- A2) methods that rely on mixed-effects models, namely PRC and DynForest, typically outperform the MFPCA-based methods (MFPCox and FunRSF);
- A3) conditionally on the method (LMM, or MFPCA) used to summarize the longitudinal predictors, the methods that use a Cox model for the survival outcome (PRC and MFPCox) outperform the corresponding methods that use a RSF (DynForest and FunRSF);
- A4) overall, the approach used to model the longitudinal predictors has a stronger

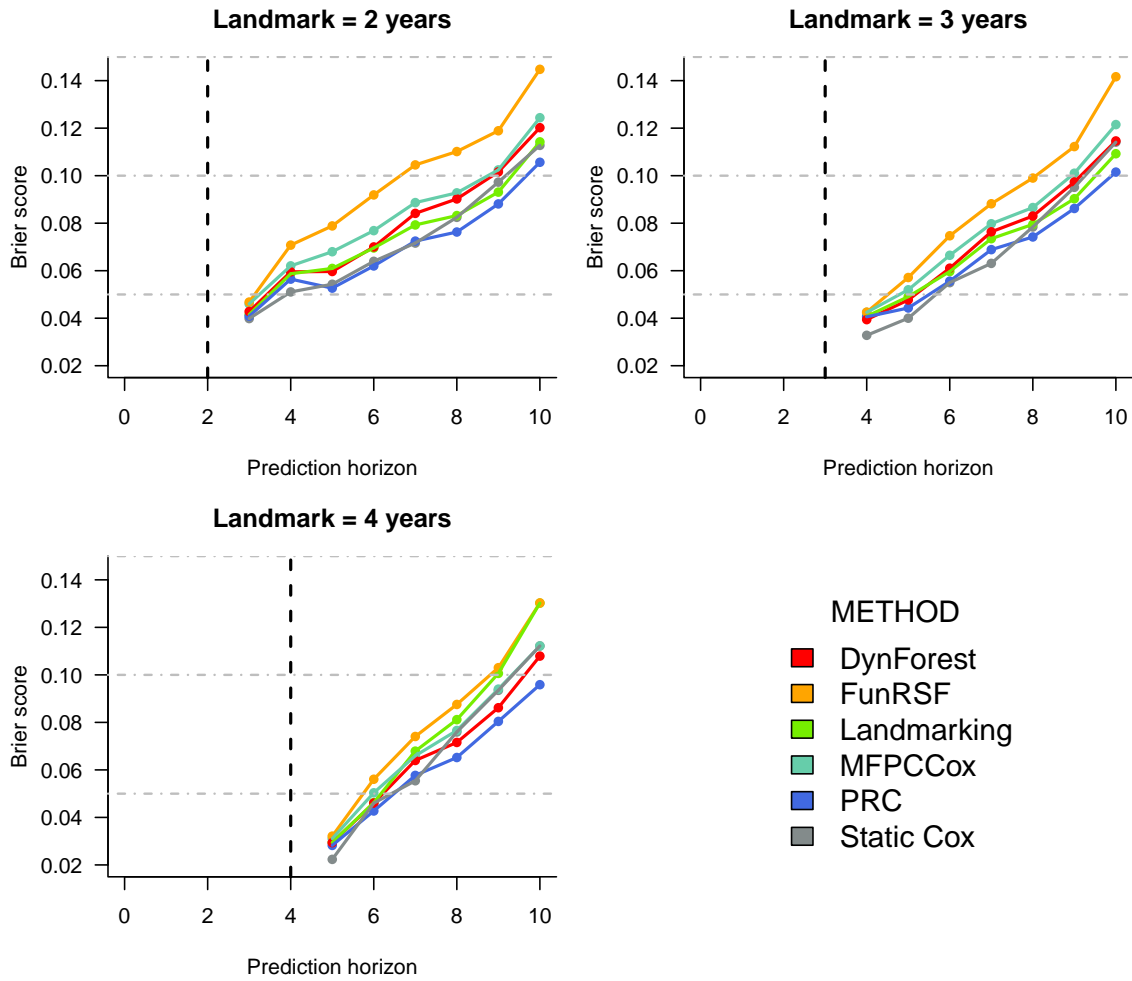


Figure 2: Cross-validated Brier score estimates for the prediction of time to dementia in the ADNI dataset. The corresponding numeric values can be found in Supplementary Table 6.

effect on predictive performance than the approach used to model the survival outcome.

4.2 ROSMAP

The repeated CV estimates of the C index, tdAUC and Brier score for the application to the ROSMAP data are presented in Table 2 and in Figures 3 and 4. At landmarks 2 and 5, no results were produced for DynForest due to the fact that estimation of this model failed on all or most (100 and 97 / 100, respectively) folds during the repeated CV. Similarly, at landmark 4 no results are presented for MFPCox and FunRSF as computation of the MFPCA scores failed on 97 of the 100 folds. These convergence issues are due to a higher percentage of missing visit / values in this dataset, that complicates the modelling of the longitudinal predictors.

C index. PRC and LOCF landmarking appear to be the best performing methods according to the estimates of the C index (Table 2). The difference in performance between the two methods is negligible at landmark 2, and slightly higher at later landmarks. MFPCox ranks third at landmarks 2 to 4, and fourth at landmark 6; DynForest ranks fourth at landmarks 3 and 4, and third at landmark 6. FunRSF and the Static Cox model exhibit the worse predictive performance.

Method	Landmark				
	2	3	4	5	6
Static Cox	0.824 (0.003)	0.812 (0.003)	0.811 (0.003)	0.799 (0.005)	0.786 (0.004)
Landmarking	0.844 (0.002)	0.849 (0.002)	0.851 (0.001)	0.854 (0.001)	0.86 (0.001)
MFPCox	0.837 (0.003)	0.845 (0.007)	0.843 (0.027)	-	0.842 (0.026)
PRC	0.846 (0.001)	0.857 (0.001)	0.864 (0.002)	0.862 (0.001)	0.868 (0.002)
FunRSF	0.806 (0.002)	0.815 (0.005)	0.814 (0.024)	-	0.808 (0.022)
DynForest	-	0.835 (0.027)	0.836 (0.018)	-	0.853 (0.003)

Table 2: Cross-validated C index estimates (and standard deviation) for the ROSMAP dataset.

Time-dependent AUC. The tdAUC estimates show that the difference in performance across methods is larger at the later landmark times. At landmark 2, PRC and landmarking achieve the highest tdAUC, followed by MFPCox. At landmark 3, DynForest has the highest tdAUC at prediction times 4 to 6, and PRC at times 7 to 15. At landmark 4, PRC has the highest tdAUC at all prediction times and is followed by DynForest, landmarking and MFPCox. At landmark 6, PRC, landmarking and DynForest clearly outperform the other 3 methods.

Brier score. Similarly to the tdAUC, also for the Brier score estimates (Table 4) the difference in performance across methods increases with the landmark. At all landmarks, PRC, landmarking, MFPCox and DynForest outperform the static Cox model and FunRSF. The difference between these methods is more visible at landmarks 3 and 4, where PRC has the lowest Brier score, DynForest the highest, and landmarking and MFPCox lay in between the two.

Summary. Differently from the ADNI dataset, in this case the Static Cox model exhibits a much worse predictive performance. This seems to indicate that for the

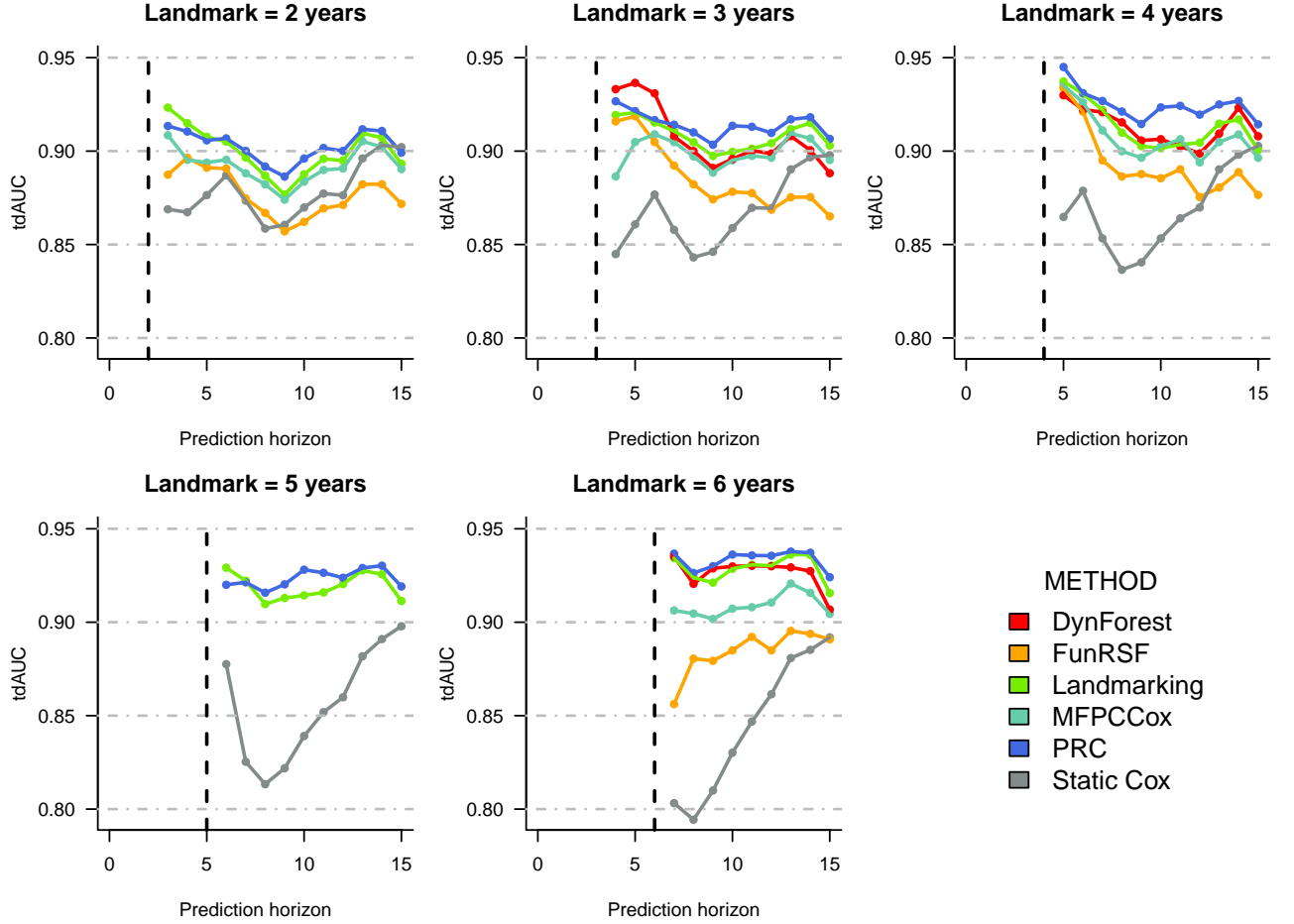


Figure 3: Cross-validation estimates of the time-dependent AUC for the prediction of time to AD in the ROSMAP dataset. The corresponding numeric values can be found in Supplementary Table 7.

ROSMAP dataset, using repeated measurement data can improve predictive performance considerably. Once again, landmarking exhibits a good predictive performance, usually ranking between second and fourth best performing method. PRC is typically first, and MFPCox and DynForest between second and fourth depending on the performance measure and landmark.

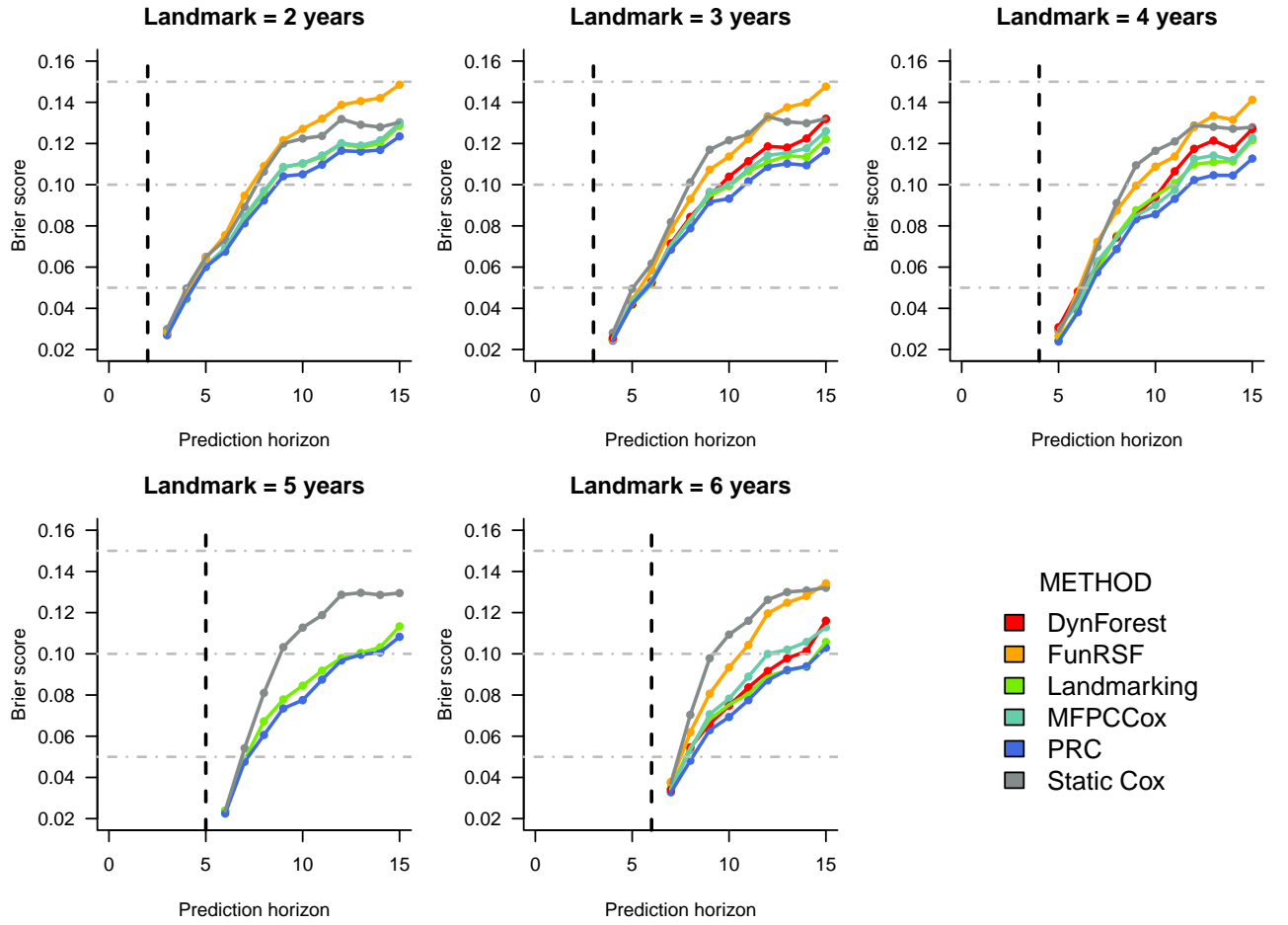


Figure 4: Cross-validated Brier score estimates for the prediction of time to AD in the ROSMAP dataset. The corresponding numeric values can be found in Supplementary Table 8.

4.3 PBC2

The repeated CV estimates of the C index, tdAUC and Brier score for the PBC2 dataset are presented in Table 3 and in Figures 5 and 6.

C index. At all landmark times, PRC achieves the highest value of the C index (Table 3); surprisingly, at landmarks 2.5 and 3 the static Cox model is the second best performing method according to this metric, and at landmark 3.5 the third. Landmarking and DynForest are next, followed by MFPCox and, last, FunRSF. The standard error of the C index estimates for this dataset is typically larger than for the ADNI and ROSMAP datasets: a result, this, that can be ascribed to the smaller sample size available in the PBC2 study to evaluate predictive performance.

Method	Landmark		
	2.5	3	3.5
Static Cox	0.813 (0.007)	0.791 (0.007)	0.788 (0.01)
Landmarking	0.798 (0.009)	0.782 (0.011)	0.796 (0.016)
MFPCox	0.753 (0.022)	0.786 (0.041)	0.781 (0.038)
PRC	0.826 (0.011)	0.809 (0.01)	0.821 (0.009)
FunRSF	0.76 (0.017)	0.732 (0.05)	0.749 (0.035)
DynForest	0.796 (0.012)	0.766 (0.009)	0.782 (0.015)

Table 3: Cross-validated C index estimates (and standard deviation) for the PBC2 dataset.

Time-dependent AUC. PRC achieves the highest tdAUC values at all landmarks. At landmark 2 it is followed by the Static Cox model, DynForest and LOCF landmarking; FunRSF and MFPCox have considerably lower predictive accuracy. At landmark 3, DynForest, LOCF landmarking and MFPCox achieve similar tdAUC values. At landmark 3.5, the trends are somewhat harder to extrapolate. It’s interesting to note that at all landmarks, the performance of the static Cox model deteriorates quickly as the prediction horizon increases. Moreover, for the first time we can observe that at landmark 2.5, FunRSF outperforms MFPCox.

Brier score. At landmark 2.5, the estimated Brier scores for landmarking, static Cox, PRC and DynForest are very similar, specially at the earlier prediction horizons. The two methods that rely on MFPCA are once again outperformed by all other methods. At landmark 3, the static Cox model has lower Brier score for predictions after 1 and 2 years from the landmark, and PRC for predictions from 3 years from the landmark onwards. At landmark 3.5, the differences between methods tend to be small for horizons at 4.5 and 5.5 years, after which the lowest Brier scores are achieved by landmarking and PRC, and the highest by FunRSF and the static Cox model.

Summary. The estimates of predictive performance for the PBC2 study are generally less accurate than for the ADNI and ROSMAP datasets due to the smaller sample size. Despite this, the results are somewhat similar to those obtained on the previous two studies.

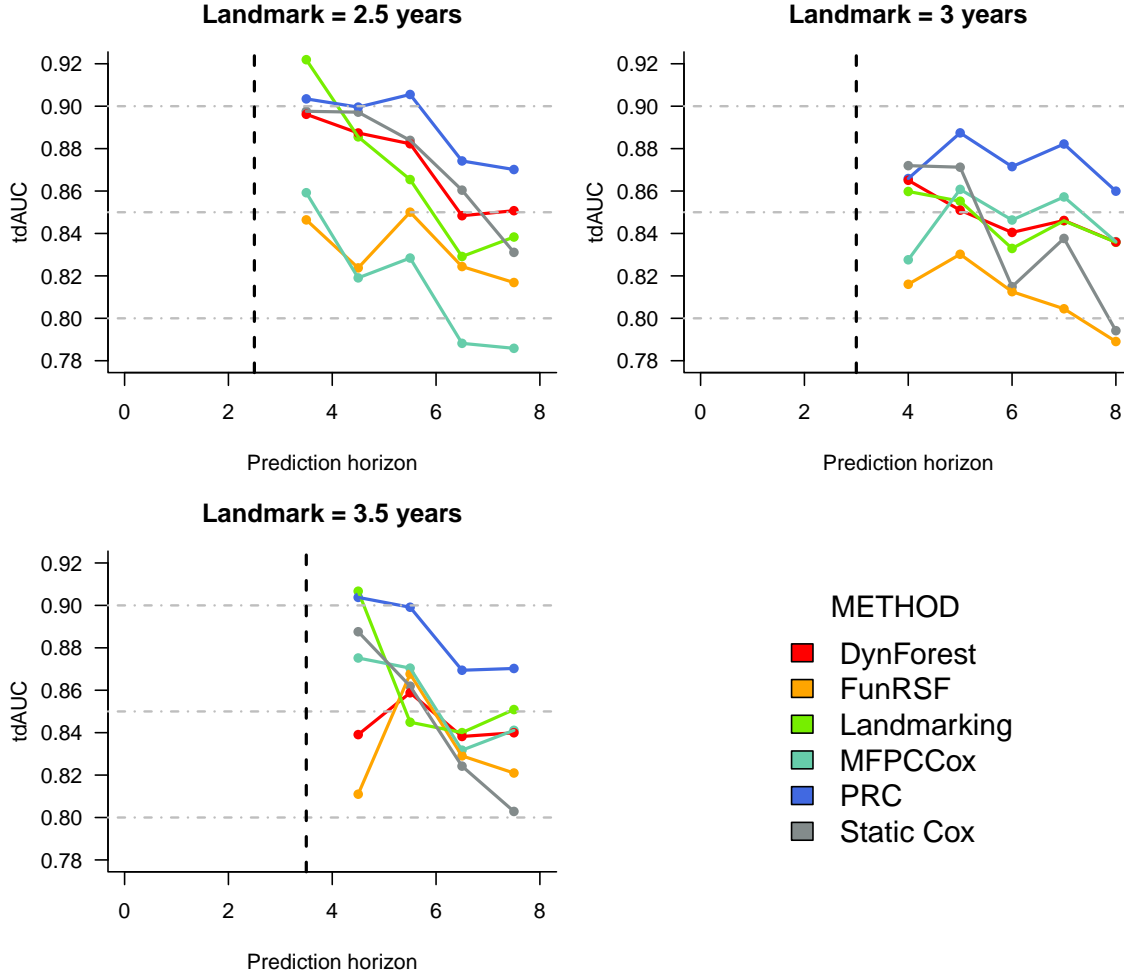


Figure 5: Cross-validation estimates of the time-dependent AUC for the prediction of time to death in the PBC2 dataset. The corresponding numeric values can be found in Supplementary Table 9.

4.4 Computing time

To give an idea of how much computing time differs across methods, the average computing time required to estimate each model in $k-1$ folds and to obtain predictions for the remaining fold during the RCV process is shown in Supplementary Tables 11-13. It can be observed that computing time typically increases with the sample size, and slightly decreases as the landmark increases (because less individuals are still at risk at later landmark times).

Estimation of models that do not model the longitudinal data, i.e. the static Cox and LOCF landmarking models, is almost immediate: this is due to the fact that these approaches only require to estimate a Cox model through R's function `coxph()`.

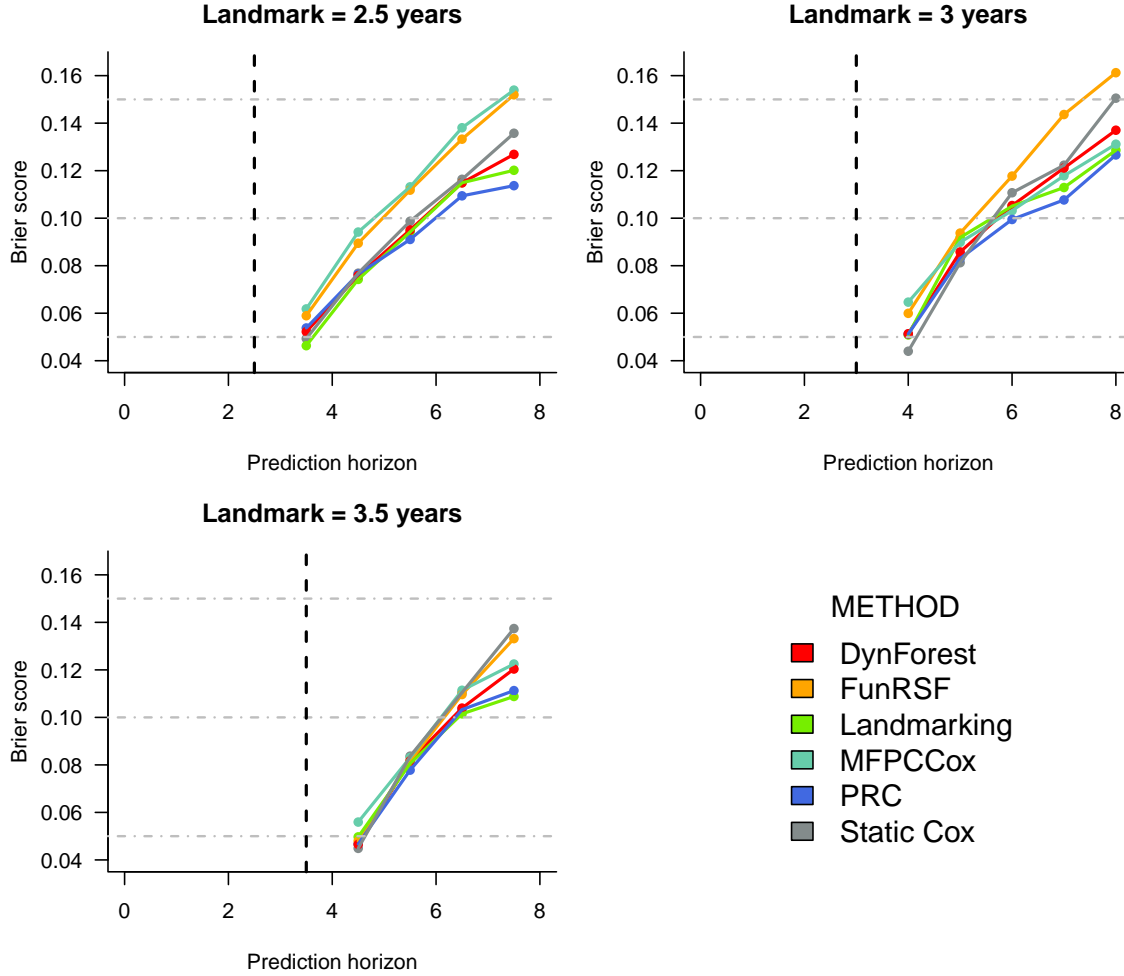


Figure 6: Cross-validated Brier score estimates for the prediction of time to death in the PBC2 dataset. The corresponding numeric values can be found in Supplementary Table 10.

Among the other methods, MFPCoX is the fastest method, followed by FunRSF: both methods can be estimated in less than a minute on all datasets. PRC and DynForest are more computationally intensive: on average, estimating PRC takes 0.57 minutes on ADNI, 1.65 minutes on ROSMAP and 7.7 seconds on PBC2; DynForest takes almost 10 minutes on ADNI, 21.1 minutes on ROSMAP and 2.5 minutes on PBC2.

5 Discussion

In this study we reviewed and evaluated the predictive performance of four recently-proposed dynamic prediction methods (MFPCoX, PRC, FunRSF, and DynForest)

that are capable of using numerous longitudinal predictors to predict survival. Each method uses a different combination of MFPCA or LMMs to model the longitudinal predictors, and of Cox model or RSF to predict the survival outcome: therefore, by comparing these methods we can also get a feeling of the extent to which the choices of using MFPCA or LMMs, and a Cox model or a RSF, can affect predictive performance. These 4 methods were further compared to a static Cox model that does not use any information after baseline, and to the LOCF landmarking approach.

Our results show that methods that use LMMs (PRC and DynForest) clearly outperform methods that use MFPCA (MFPC Cox and FunRSF) to model the trajectories of the longitudinal covariates. PRC is frequently the best performing method with respect to the different metrics considered; it is usually followed by DynForest and MFPC Cox, while FunRSF almost always exhibits the worst predictive performance.

As concerns the method used to predict survival, it seems that on the datasets considered in this study, using a Cox model allows to achieve a better predictive performance than using a RSF, as highlighted by the fact that conditionally on the same method used to model the longitudinal predictors, PRC outperforms DynForest and MFPC Cox outperforms FunRSF. Interestingly, LOCF landmarking often showed a good predictive performance, pointing out how such a simple and intuitive prediction method can often deliver good predictions of survival.

When considering computing time, most methods proved to be quite fast to estimate. DynForest was by far the most time-consuming method: this can be attributed to the fact that instead of estimating LMMs once, DynForest re-estimates the LMMs after each node split. Besides increasing computing time, this can also lead to more frequent convergence problems. Another method that took longer was PRC, showing how in general, estimation of LMMs is more time-consuming than estimation of the MFPCA scores. Nevertheless, using LMMs clearly resulted in higher predictive accuracy, justifying the increased computing time.

The main advantage of the two-step methods considered in this study is that they make it possible to extend the applicability of dynamic prediction to studies with tens, hundreds or (potentially) even hundreds of longitudinal covariates. At the same time, these new methods lack some elements of flexibility:

- To be able to estimate the MFPCA scores, with MFPC Cox and FunRSF it was necessary to standardize the measurement times across subjects so as to have a shared time grid. This is undesirable, both for longitudinal studies with fixed measurement times, where individual visits may deviate from the planned date, and for longitudinal studies where there is no planned visit schedule;
- DynForest and PRC are limited to LMMs. This induced us to apply skewness-reducing transformations to strongly-skewed longitudinal predictors so as to reduce convergence problems; moreover, in the case of discrete predictors it would be preferable to resort to GLMMs;

- none of the 4 methods currently allows to deal with interval censoring, which is common in longitudinal studies;
- MFPCox, FunRSF and PRC don't allow to model competing risks.

All four methods require users to make choices about tuning parameters. This is less of a problem with PRC, that uses cross-validation to select the value(s) of the penalty parameter(s), and with MFPCox, where one only needs to choose the percentage of variance explained that the MFPCA scores need to retain. In addition to the percentage of variance explained, FunRSF also requires the specification of the number of variables to choose as candidates for node splitting, and of the minimal number of subjects that a terminal node needs to contain. DynForest requires users to specify three tuning parameters: number of candidate covariates, and number of subjects and of events that determine the termination of node splitting.

Finally, PRC and DynForest come with software implementations (Signorelli, 2023; Devaux et al., 2023) that make it easy for users to implement those methods. MFPCox and FunRSF, instead, lack a proper software implementation, forcing users to adapt the code presented in the corresponding publications to their own datasets.

Supplementary tables and figures

Supplementary tables and figures are available in the “Supplementary Material” pdf file.

Data availability

ROSMAP. The data from the ROSMAP study are available upon motivated request from the Rush Alzheimer’s Disease Center (RADC) of the RUSH University. ROSMAP resources can be requested at <https://www.radc.rush.edu> and www.synapse.org. All ROSMAP participants enrolled without known dementia and agreed to detailed clinical evaluation and brain donation at death (Bennett et al., 2018). The ROS and MAP studies were approved by an Institutional Review Board of Rush University Medical Center. Each participant signed an informed consent, Anatomic Gift Act, and repository consent to allow their data to be repurposed.

ADNI. The ADNI data are available upon motivated request from the Alzheimer’s Disease Neuroimaging Initiative (ADNI) database (<http://adni.loni.usc.edu>).

PBC2. The PBC2 dataset is publicly available and can be found in several R packages including, among others, `DynForest`, `joineRML` and `pencal`.

Acknowledgements

ROSMAP. ROSMAP is supported by P30AG10161, P30AG72975, R01AG15819, R01AG17917, U01AG46152, and U01AG61356.

ADNI. Data from the ADNI study were obtained from the ADNI database (<http://adni.loni.usc.edu>). As such, the investigators within the ADNI contributed to the design and implementation of ADNI and/or provided data but did not participate in analysis or writing of this paper. A complete listing of ADNI investigators can be found at https://adni.loni.usc.edu/wp-content/uploads/how_to_apply/ADNI_Acknowledgement_List.pdf. Data from the ROSMAP study were obtained from the Rush Alzheimer’s Disease Center (RADC) of the RUSH University (<https://www.radc.rush.edu>).

References

- Bennett, D. A., Buchman, A. S., Boyle, P. A., Barnes, L. L., Wilson, R. S., and Schneider, J. A. (2018). Religious Orders Study and Rush Memory and Aging Project. *Journal of Alzheimer’s Disease*, 64(s1):S161–S189.
- Cox, D. R. (1972). Regression models and life-tables. *Journal of the Royal Statistical Society: Series B (Methodological)*, 34(2):187–202.
- Devaux, A., Helmer, C., Dufouil, C., Genuer, R., and Proust-Lima, C. (2022). Random survival forests for competing risks with multivariate longitudinal endogenous covariates. *arXiv preprint arXiv:2208.05801*.
- Devaux, A., Proust-Lima, C., and Genuer, R. (2023). Random Forests for time-fixed and time-dependent predictors: The DynForest R package. *arXiv preprint arXiv:2302.02670*.
- Filbin, M. R., Mehta, A., Schneider, A. M., Kays, K. R., Guess, J. R., Gentili, M., Fenyves, B. G., Charland, N. C., Gonye, A. L., Gushterova, I., et al. (2021). Longitudinal proteomic analysis of severe covid-19 reveals survival-associated signatures, tissue-specific cell death, and cell-cell interactions. *Cell Reports Medicine*, 2(5).
- Gomon, D., Putter, H., Fiocco, M., and Signorelli, M. (2024). Dynamic prediction of survival using multivariate functional principal component analysis: A strict land-marking approach. *Statistical Methods in Medical Research*.
- Graf, E., Schmoor, C., Sauerbrei, W., and Schumacher, M. (1999). Assessment and comparison of prognostic classification schemes for survival data. *Statistics in Medicine*, 18(17-18):2529–2545.
- Happ, C. and Greven, S. (2018). Multivariate functional principal component analysis for data observed on different (dimensional) domains. *Journal of the American Statistical Association*, 113(522):649–659.
- Heagerty, P. J., Lumley, T., and Pepe, M. S. (2000). Time-dependent ROC curves for censored survival data and a diagnostic marker. *Biometrics*, 56(2):337–344.

- Iswaran, H., Kogalur, U., Blackstone, E., and Lauer, M. (2008). Random survival forests. *The Annals of Applied Statistics*, 2(3):841–860.
- Li, K. and Luo, S. (2019). Dynamic prediction of Alzheimer’s Disease progression using features of multiple longitudinal outcomes and time-to-event data. *Statistics in Medicine*, 38(24):4804–4818.
- Lin, J., Li, K., and Luo, S. (2021). Functional survival forests for multivariate longitudinal outcomes: Dynamic prediction of Alzheimer’s disease progression. *Statistical Methods in Medical Research*, 30(1):99–111.
- McCulloch, C. E. and Searle, S. R. (2004). *Generalized, Linear, and Mixed Models*. John Wiley & Sons.
- Murtaugh, P. A., Dickson, E. R., Van Dam, G. M., Malinchoc, M., Grambsch, P. M., Langworthy, A. L., and Gips, C. H. (1994). Primary biliary cirrhosis: prediction of short-term survival based on repeated patient visits. *Hepatology*, 20(1):126–134.
- Patel, A. V., Jacobs, E. J., Dudas, D. M., Briggs, P. J., Lichtman, C. J., Bain, E. B., Stevens, V. L., McCullough, M. L., Teras, L. R., Campbell, P. T., et al. (2017). The american cancer society’s cancer prevention study 3 (cps-3): recruitment, study design, and baseline characteristics. *Cancer*, 123(11):2014–2024.
- Pencina, M. J. and D’Agostino, R. B. (2004). Overall C as a measure of discrimination in survival analysis: model specific population value and confidence interval estimation. *Statistics in Medicine*, 23(13):2109–2123.
- Putter, H. and van Houwelingen, H. C. (2022). Landmarking 2.0: Bridging the gap between joint models and landmarking. *Statistics in Medicine*, 41(11):1901–1917.
- Rizopoulos, D. (2012). *Joint models for longitudinal and time-to-event data*. CRC press.
- Signorelli, M. (2023). pencial: an R package for the Dynamic Prediction of Survival with Many Longitudinal Predictors. *arXiv preprint arXiv:2309.15600*.
- Signorelli, M., Ayoglu, B., Johansson, C., Lochmüller, H., Straub, V., Muntoni, F., Niks, E., Tsonaka, R., Persson, A., Aartsma-Rus, A., et al. (2020). Longitudinal serum biomarker screening identifies malate dehydrogenase 2 as candidate prognostic biomarker for Duchenne muscular dystrophy. *Journal of Cachexia, Sarcopenia and Muscle*, 11(2):505–517.
- Signorelli, M., Spitali, P., Szegedy, C. A.-K., Consortium, M.-M., and Tsonaka, R. (2021). Penalized regression calibration: A method for the prediction of survival outcomes using complex longitudinal and high-dimensional data. *Statistics in Medicine*, 40(27):6178–6196.

- Steyerberg, E. W. (2009). *Clinical Prediction Models*. Springer.
- Therneau, T. M. and Grambsch, P. M. (2000). *Modeling survival data: extending the Cox model*. Springer.
- Van Houwelingen, H. C. (2007). Dynamic prediction by landmarking in event history analysis. *Scandinavian Journal of Statistics*, 34(1):70–85.
- Weiner, M. W., Aisen, P. S., Jack Jr, C. R., Jagust, W. J., Trojanowski, J. Q., Shaw, L., Saykin, A. J., Morris, J. C., Cairns, N., Beckett, L. A., et al. (2010). The Alzheimer’s disease neuroimaging initiative: progress report and future plans. *Alzheimer’s & Dementia*, 6(3):202–211.

Supplementary material for the article:
“An empirical appraisal of methods for the dynamic
prediction of survival with many longitudinal predictors”

Mirko Signorelli¹ and Sophie Retif²

¹*Mathematical Institute, Leiden University (NL)*

²*School of Industrial and Information Engineering, Politecnico di Milano (IT)*

Contents

1	Supplementary tables	1
2	Supplementary figures	11

1 Supplementary tables

Variable name	Description	Variable type
ADAS11	Alzheimer's Disease Assessment Scale (ADAS) 11	Continuous
ADAS13	ADAS 13	Continuous
ADASQ4	ADAS Delayed Word Recall	Discrete
CDRSB	Clinical Dementia Rating scale Sum of Boxes	Discrete
Entorhinal	University of California, San Francisco (UCSF) Entorhinal	Continuous
FAQ	FAQ	Discrete
Fusiform	UCSF Fusiform	Continuous
Hippocampus	UCSF Hippocampus	Continuous
ICV	UCSF ICV	Continuous
LDELTOTAL	Logical Memory - Delayed Recall	Discrete
MidTemp	UCSF Middle temporal gyrus	Continuous
MMSE	MMSE	Discrete
mPACCdigit	ADNI-modified Preclinical Alzheimer's Cognitive Composite (PACC) with Digit Symbol Substitution	Continuous
mPACCtrailsB	ADNI-modified PACC with Trails B	Continuous
RAVLT.forgetting	Rey Auditory Verbal Learning Test (RAVLT) Forgetting	Discrete
RAVLT.immediate	RAVLT Immediate	Discrete
RAVLT.learning	RAVLT Learning	Continuous
RAVLT.perc.forgetting	RAVLT Percent Forgetting	Continuous
TRABSCOR	Trails B	Continuous
Ventricles	UCSF Ventricles	Continuous
WholeBrain	UCSF WholeBrain	Continuous

Table 1: List of longitudinal covariates used as predictors for the ADNI dataset.

Variable name	Description	Variable type
bmi	Body mass index	Continuous
bradysc	Bradykinesia score	Discrete
cesdsum	Depressive symptoms	Discrete
cogn_ep	Episodic memory	Continuous
cogn_global	Global cognitive function	Continuous
cogn_po	Perceptual orientation	Continuous
cogn_ps	Perceptual speed	Continuous
cogn_se	Semantic memory	Continuous
cogn_wo	Working memory	Continuous
d_frailty	Frailty	Discrete
dbp_avg	Diastolic blood pressure	Continuous
gaitsc	Gait score	Continuous
iadlsum	Instrumental activities of daily living	Discrete
katzsum	Basic activities of daily living	Discrete
motor_dexterity	Motor dexterity	Continuous
motor_gait	Motor gait	Continuous
motor_handstreng	Motor hand strength	Continuous
motor10	Motor function	Continuous
parkinsonism_tri	Parkinsonism	Discrete
phys5itemsum	Physical activity	Continuous
r_depres	Clinical depression	Discrete
r_pd	Clinical Parkinson's disease	Discrete
r_stroke	Stroke diagnosis	Discrete
rigidsc	Rigidity score	Discrete
rosbsum	Mobility disability	Discrete
sbp_avg	Systolic blood pressure	Continuous
soc_net	Social network size	Continuous
tremsc	Tremor score	Continuous
vasc_risks_sum	Vascular disease risk factors	Continuous
vision	Visual acuity	Discrete

Table 2: List of longitudinal covariates used as predictors for the ROSMAP dataset.

Variable name	Description	Variable type
albumin	Albumin	Continuous
alkaline	Alkaline phosphatase	Continuous
histologic	Histologic stage of disease	Discrete
platelets	Platelets	Continuous
prothrombin	Prothrombin time	Continuous
serBilir	Serum bilirubin	Continuous
serChol	Serum cholesterol	Continuous
SGOT	Serum glutamic-oxaloacetic transaminase	Continuous

Table 3: List of longitudinal covariates used as predictors for the PBC2 dataset.

Estimation attempt	ADNI	ROSMAP	PBC2
First	5	15	4
Second	10	20	6
Third	15	25	8
Fourth	20	30	10

Table 4: Value of s (`nodesize` parameter in the `DynForest` package) used to estimate the trees within the RSFs of `DynForest` at the first, second, third and fourth estimation attempt.

Landmark = 2 years								
Horizon	3	4	5	6	7	8	9	10
DynForest	0.931	0.940	0.948	0.933	0.916	0.917	0.901	0.887
FunRSF	0.923	0.924	0.930	0.915	0.892	0.893	0.885	0.848
Landmarking	0.943	0.943	0.954	0.944	0.934	0.935	0.917	0.895
MFPCox	0.924	0.936	0.937	0.922	0.907	0.904	0.889	0.873
PRC	0.947	0.952	0.967	0.950	0.940	0.942	0.924	0.907
Static Cox	0.927	0.942	0.946	0.937	0.931	0.915	0.895	0.889

Landmark = 3 years							
Horizon	4	5	6	7	8	9	10
DynForest	0.937	0.944	0.923	0.898	0.905	0.891	0.891
FunRSF	0.927	0.934	0.905	0.884	0.878	0.872	0.831
Landmarking	0.922	0.943	0.929	0.909	0.908	0.901	0.878
MFPCox	0.927	0.926	0.906	0.896	0.889	0.878	0.862
PRC	0.948	0.962	0.945	0.927	0.931	0.917	0.915
Static Cox	0.934	0.946	0.929	0.921	0.888	0.868	0.862

Landmark = 4 years						
Horizon	5	6	7	8	9	10
DynForest	0.947	0.918	0.898	0.906	0.893	0.882
FunRSF	0.939	0.920	0.889	0.884	0.872	0.834
Landmarking	0.909	0.902	0.885	0.895	0.871	0.851
MFPCox	0.930	0.910	0.891	0.898	0.875	0.844
PRC	0.960	0.939	0.927	0.938	0.922	0.908
Static Cox	0.939	0.913	0.906	0.871	0.853	0.855

Table 5: Cross-validation estimates of the time-dependent AUC for the ADNI dataset

Landmark = 2 years								
Horizon	3	4	5	6	7	8	9	10
DynForest	0.043	0.060	0.060	0.070	0.084	0.090	0.102	0.120
FunRSF	0.047	0.071	0.079	0.092	0.105	0.110	0.119	0.145
Landmarking	0.042	0.059	0.061	0.070	0.079	0.083	0.093	0.114
MFPCox	0.046	0.062	0.068	0.077	0.089	0.093	0.102	0.124
PRC	0.041	0.056	0.053	0.062	0.072	0.076	0.088	0.106
Static Cox	0.040	0.051	0.054	0.064	0.072	0.082	0.097	0.113

Landmark = 3 years							
Horizon	4	5	6	7	8	9	10
DynForest	0.039	0.048	0.061	0.076	0.083	0.097	0.115
FunRSF	0.043	0.057	0.075	0.088	0.099	0.112	0.142
Landmarking	0.041	0.049	0.060	0.073	0.080	0.090	0.109
MFPCox	0.042	0.052	0.066	0.080	0.087	0.101	0.122
PRC	0.041	0.044	0.056	0.069	0.074	0.086	0.102
Static Cox	0.033	0.040	0.055	0.063	0.078	0.095	0.114

Landmark = 4 years						
Horizon	5	6	7	8	9	10
DynForest	0.029	0.046	0.064	0.072	0.086	0.108
FunRSF	0.032	0.056	0.074	0.088	0.103	0.130
Landmarking	0.029	0.046	0.068	0.081	0.101	0.130
MFPCox	0.031	0.050	0.066	0.077	0.094	0.112
PRC	0.028	0.043	0.058	0.065	0.080	0.096
Static Cox	0.022	0.046	0.055	0.076	0.093	0.112

Table 6: Cross-validated Brier score estimates for the ADNI dataset

Landmark = 2 years													
Horizon	3	4	5	6	7	8	9	10	11	12	13	14	15
FunRSF	0.887	0.896	0.891	0.891	0.875	0.867	0.857	0.862	0.869	0.871	0.882	0.882	0.872
Landmarking	0.923	0.915	0.908	0.905	0.897	0.887	0.877	0.888	0.896	0.895	0.909	0.907	0.893
MFPCox	0.909	0.895	0.894	0.895	0.888	0.882	0.874	0.884	0.890	0.891	0.905	0.902	0.890
PRC	0.913	0.910	0.906	0.907	0.900	0.892	0.886	0.896	0.902	0.900	0.912	0.911	0.899
Static Cox	0.869	0.867	0.876	0.887	0.874	0.859	0.861	0.870	0.877	0.876	0.896	0.903	0.902

Landmark = 3 years												
Horizon	4	5	6	7	8	9	10	11	12	13	14	15
DynForest	0.933	0.937	0.931	0.908	0.900	0.891	0.896	0.900	0.899	0.908	0.900	0.888
FunRSF	0.916	0.919	0.905	0.892	0.882	0.874	0.878	0.878	0.869	0.875	0.875	0.865
Landmarking	0.919	0.921	0.915	0.911	0.905	0.897	0.900	0.901	0.904	0.912	0.915	0.903
MFPCox	0.886	0.905	0.909	0.905	0.897	0.888	0.895	0.897	0.896	0.909	0.907	0.895
PRC	0.927	0.921	0.917	0.914	0.910	0.903	0.914	0.913	0.910	0.917	0.918	0.907
Static Cox	0.845	0.861	0.877	0.858	0.843	0.846	0.859	0.870	0.869	0.890	0.897	0.898

Landmark = 4 years											
Horizon	5	6	7	8	9	10	11	12	13	14	15
DynForest	0.930	0.922	0.921	0.915	0.906	0.906	0.903	0.899	0.909	0.923	0.908
FunRSF	0.934	0.921	0.895	0.886	0.888	0.885	0.890	0.875	0.881	0.889	0.877
Landmarking	0.937	0.931	0.922	0.910	0.903	0.902	0.903	0.905	0.915	0.917	0.901
MFPCox	0.935	0.926	0.911	0.900	0.896	0.903	0.906	0.894	0.905	0.909	0.896
PRC	0.945	0.931	0.927	0.921	0.914	0.923	0.924	0.920	0.925	0.927	0.914
Static Cox	0.865	0.879	0.853	0.836	0.840	0.853	0.864	0.870	0.890	0.898	0.903

Landmark = 5 years										
Horizon	6	7	8	9	10	11	12	13	14	15
Landmarking	0.929	0.922	0.910	0.913	0.914	0.916	0.920	0.928	0.926	0.911
PRC	0.920	0.921	0.916	0.920	0.928	0.926	0.924	0.929	0.930	0.919
Static Cox	0.878	0.825	0.813	0.822	0.839	0.852	0.860	0.882	0.891	0.898

Landmark = 6 years									
Horizon	7	8	9	10	11	12	13	14	15
DynForest	0.935	0.921	0.929	0.930	0.930	0.930	0.929	0.927	0.907
FunRSF	0.856	0.881	0.879	0.885	0.892	0.885	0.895	0.894	0.891
Landmarking	0.934	0.924	0.921	0.929	0.931	0.930	0.936	0.936	0.916
MFPCox	0.906	0.905	0.902	0.907	0.908	0.911	0.921	0.916	0.904
PRC	0.937	0.926	0.930	0.936	0.936	0.936	0.938	0.937	0.924
Static Cox	0.803	0.794	0.810	0.830	0.847	0.861	0.881	0.885	0.892

Table 7: Cross-validation estimates of the time-dependent AUC for the ROSMAP dataset

Landmark = 2 years													
Horizon	3	4	5	6	7	8	9	10	11	12	13	14	15
FunRSF	0.028	0.048	0.064	0.076	0.095	0.109	0.122	0.127	0.132	0.139	0.141	0.142	0.149
Landmarking	0.027	0.044	0.060	0.068	0.084	0.096	0.108	0.110	0.114	0.120	0.118	0.120	0.129
MFPCox	0.028	0.045	0.061	0.069	0.085	0.097	0.109	0.110	0.114	0.120	0.119	0.122	0.130
PRC	0.027	0.045	0.060	0.068	0.081	0.092	0.104	0.105	0.110	0.117	0.116	0.117	0.123
Static Cox	0.030	0.050	0.065	0.073	0.089	0.106	0.120	0.122	0.124	0.132	0.129	0.128	0.130

Landmark = 3 years												
Horizon	4	5	6	7	8	9	10	11	12	13	14	15
DynForest	0.026	0.042	0.053	0.072	0.084	0.095	0.104	0.111	0.119	0.118	0.122	0.132
FunRSF	0.025	0.044	0.059	0.078	0.093	0.107	0.114	0.122	0.133	0.138	0.140	0.148
Landmarking	0.025	0.042	0.052	0.071	0.083	0.095	0.099	0.106	0.111	0.114	0.113	0.122
MFPCox	0.025	0.044	0.053	0.071	0.083	0.097	0.100	0.108	0.114	0.115	0.118	0.126
PRC	0.024	0.042	0.053	0.068	0.079	0.092	0.093	0.102	0.109	0.110	0.109	0.117
Static Cox	0.028	0.049	0.062	0.082	0.101	0.117	0.122	0.125	0.133	0.131	0.130	0.132

Landmark = 4 years											
Horizon	5	6	7	8	9	10	11	12	13	14	15
DynForest	0.031	0.048	0.061	0.074	0.085	0.094	0.106	0.117	0.121	0.117	0.127
FunRSF	0.027	0.048	0.072	0.087	0.100	0.109	0.114	0.128	0.133	0.131	0.141
Landmarking	0.025	0.039	0.058	0.075	0.088	0.094	0.101	0.110	0.111	0.111	0.122
MFPCox	0.030	0.042	0.063	0.074	0.085	0.090	0.097	0.113	0.114	0.112	0.123
PRC	0.024	0.038	0.057	0.069	0.083	0.086	0.093	0.102	0.105	0.104	0.113
Static Cox	0.029	0.046	0.070	0.091	0.109	0.116	0.121	0.129	0.128	0.127	0.128

Landmark = 5 years										
Horizon	6	7	8	9	10	11	12	13	14	15
Landmarking	0.024	0.049	0.067	0.078	0.085	0.092	0.098	0.100	0.103	0.113
PRC	0.022	0.048	0.061	0.073	0.078	0.087	0.097	0.100	0.101	0.108
Static Cox	0.024	0.054	0.081	0.103	0.113	0.119	0.129	0.130	0.129	0.129

Landmark = 6 years									
Horizon	7	8	9	10	11	12	13	14	15
DynForest	0.034	0.055	0.066	0.075	0.084	0.092	0.098	0.101	0.116
FunRSF	0.038	0.062	0.081	0.093	0.104	0.120	0.125	0.128	0.134
Landmarking	0.035	0.054	0.068	0.075	0.081	0.089	0.092	0.094	0.106
MFPCox	0.034	0.053	0.071	0.078	0.089	0.100	0.102	0.106	0.113
PRC	0.033	0.048	0.063	0.069	0.078	0.087	0.092	0.094	0.103
Static Cox	0.037	0.070	0.098	0.109	0.116	0.126	0.130	0.131	0.132

Table 8: Cross-validated Brier score estimates for the ROSMAP dataset

Landmark = 2.5 years					
Horizon	3.5	4.5	5.5	6.5	7.5
DynForest	0.896	0.887	0.882	0.848	0.851
FunRSF	0.846	0.824	0.850	0.824	0.817
Landmarking	0.922	0.886	0.865	0.829	0.838
MFPCox	0.859	0.819	0.828	0.788	0.786
PRC	0.903	0.900	0.906	0.874	0.870
Static Cox	0.898	0.897	0.884	0.860	0.831

Landmark = 3 years					
Horizon	4	5	6	7	8
DynForest	0.865	0.851	0.840	0.846	0.836
FunRSF	0.816	0.830	0.813	0.804	0.789
Landmarking	0.860	0.855	0.833	0.846	0.836
MFPCox	0.828	0.861	0.846	0.857	0.836
PRC	0.866	0.887	0.872	0.882	0.860
Static Cox	0.872	0.871	0.815	0.838	0.794

Landmark = 3.5 years				
Horizon	4.5	5.5	6.5	7.5
DynForest	0.839	0.859	0.838	0.840
FunRSF	0.811	0.868	0.829	0.821
Landmarking	0.907	0.845	0.840	0.851
MFPCox	0.875	0.870	0.832	0.841
PRC	0.904	0.899	0.869	0.870
Static Cox	0.888	0.862	0.824	0.803

Table 9: Cross-validation estimates of the time-dependent AUC for the PBC2 dataset

Landmark = 2.5 years					
Horizon	3.5	4.5	5.5	6.5	7.5
DynForest	0.052	0.076	0.095	0.115	0.127
FunRSF	0.059	0.089	0.112	0.133	0.152
Landmarking	0.046	0.074	0.094	0.115	0.120
MFPCox	0.062	0.094	0.113	0.138	0.154
PRC	0.054	0.076	0.091	0.109	0.114
Static Cox	0.049	0.077	0.099	0.116	0.136

Landmark = 3 years					
Horizon	4	5	6	7	8
DynForest	0.051	0.086	0.105	0.121	0.137
FunRSF	0.060	0.094	0.118	0.144	0.161
Landmarking	0.051	0.092	0.105	0.113	0.129
MFPCox	0.065	0.090	0.103	0.118	0.131
PRC	0.051	0.083	0.099	0.108	0.127
Static Cox	0.044	0.081	0.111	0.122	0.151

Landmark = 3.5 years				
Horizon	4.5	5.5	6.5	7.5
DynForest	0.047	0.082	0.104	0.120
FunRSF	0.048	0.082	0.110	0.133
Landmarking	0.050	0.081	0.101	0.109
MFPCox	0.056	0.083	0.111	0.122
PRC	0.047	0.078	0.103	0.111
Static Cox	0.045	0.084	0.110	0.137

Table 10: Cross-validated Brier score estimates for the PBC2 dataset

Method	Landmark			Average
	2	3	4	
Static Cox	0.009	0.007	0.006	0.007
Landmarking	0.010	0.007	0.006	0.008
MFPCox	0.080	0.046	0.046	0.057
PRC	0.776	0.482	0.453	0.571
FunRSF	0.240	0.122	0.125	0.163
DynForest	12.501	9.077	8.099	9.892

Table 11: Average computing time per CV fold (in **minutes**) for the ADNI dataset.

Method	Landmark					Average
	2	3	4	5	6	
Static Cox	0.022	0.019	0.016	0.014	0.011	0.017
Landmarking	0.023	0.020	0.017	0.014	0.011	0.017
MFPCox	0.194	0.135	0.066	-	0.064	0.115
PRC	3.755	1.151	1.138	1.115	1.124	1.657
FunRSF	0.604	0.367	0.115	-	0.124	0.302
DynForest	-	11.504	17.657	-	34.147	21.102

Table 12: Average computing time per CV fold (in **minutes**) for the ROSMAP dataset.

Method	Landmark			Average
	2.5	3	3.5	
Static Cox	0.253	0.246	0.177	0.226
Landmarking	0.260	0.240	0.188	0.229
MFPCox	0.902	0.522	0.556	0.660
PRC	7.832	7.616	7.762	7.737
FunRSF	2.776	1.393	1.526	1.898
DynForest	186.136	136.747	128.914	150.599

Table 13: Average computing time per CV fold (in **seconds**) for the PBC2 dataset.

2 Supplementary figures

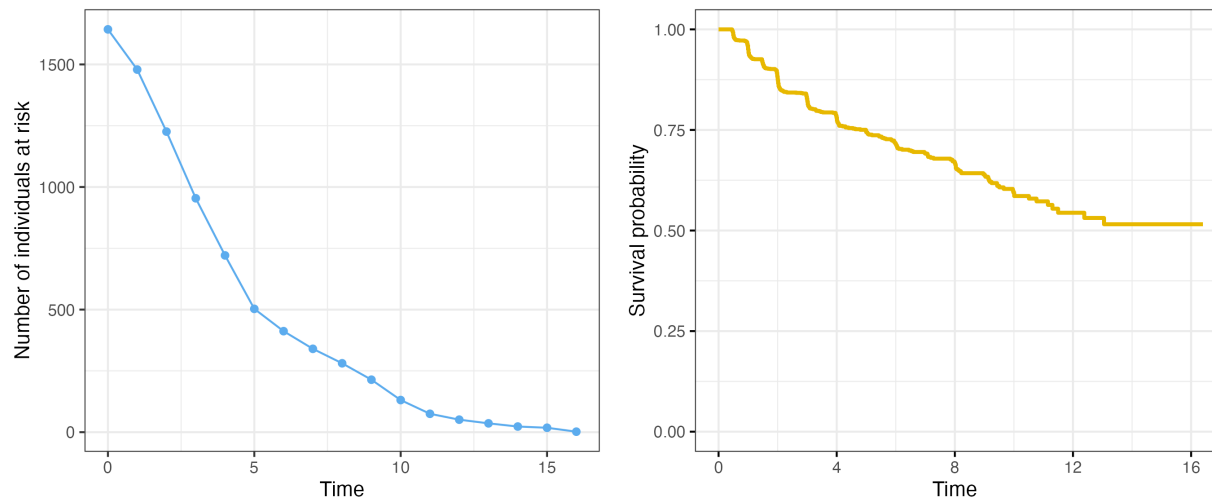


Figure 1: Number of subjects at risk (left) and Kaplan-Meier chart (right) for the ADNI dataset.

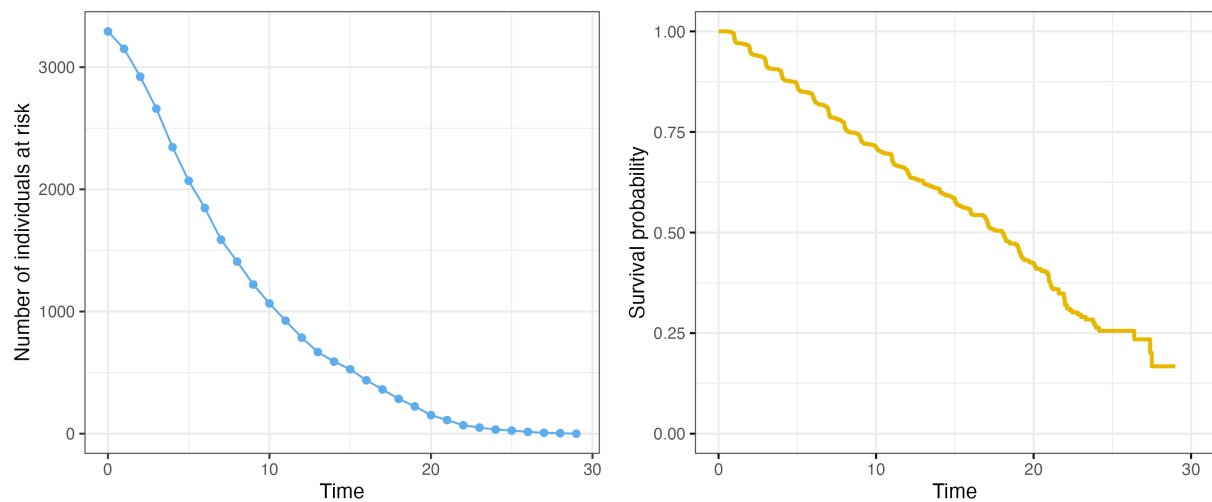


Figure 2: Number of subjects at risk (left) and Kaplan-Meier chart (right) for the ROSMAP dataset.

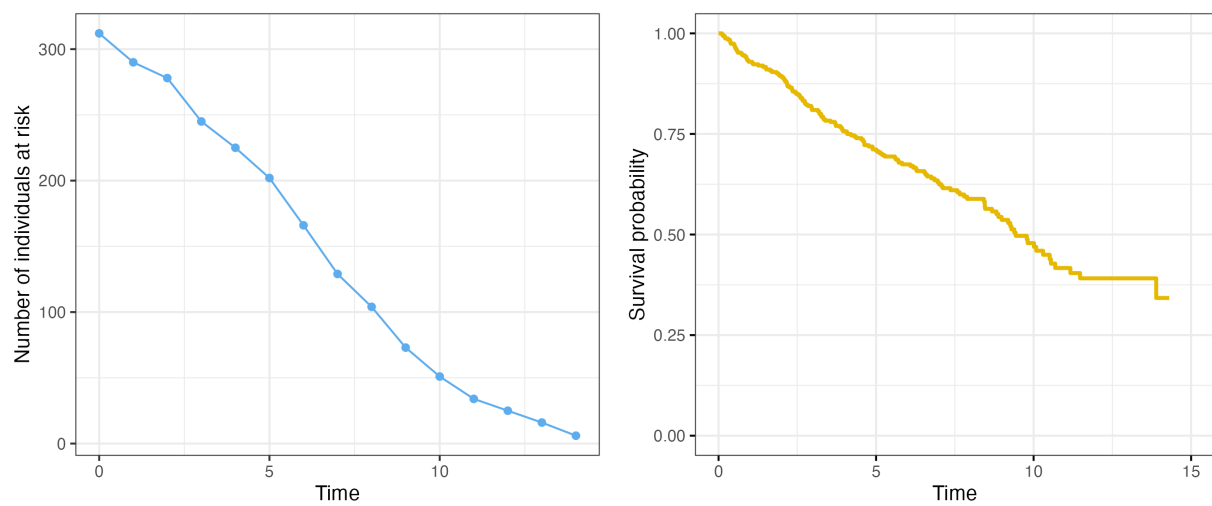


Figure 3: Number of subjects at risk (left) and Kaplan-Meier chart (right) for the PBC2 dataset.